Whole exome sequencing in the differential diagnosis of Diamond-Blackfan anemia: Clinical and molecular study of three patients with novel *RPL5* and mosaic *RPS19* mutations

CrossMark

Edoardo Errichiello [a,*], Annalisa Vetro [a], Tommaso Mina [b], Anita Wischmeijer [c,f], Enrico Berrino [d], Miriam Carella [a,e], Maria Romagnoli [f], Patrizia Sacchini [g], Tiziana Venesio [d], Marco Zecca [b], Orsetta Zuffardi [a]

[a] Department of Molecular Medicine, University of Pavia, Pavia, Italy
[b] Pediatric Hematology and Oncology, IRCCS Fondazione Policlinico S. Matteo, Pavia, Italy
[c] Genetic Counseling Service, Department of Pediatrics, Regional Hospital of Bolzano, Bolzano, Italy
[d] Unit of Molecular Pathology, Candiolo Cancer Institute, FPO-IRCCS, Candiolo, (Torino), Italy
[e] IRCCS Fondazione Policlinico S. Matteo, Pavia, Italy
[f] Unit of Medical Genetics, University of Bologna, Bologna, Italy
[g] Unit of Pediatrics, Ospedale Infermi di Rimini, Rimini, Italy

ARTICLE INFO

ABSTRACT

Diamond-Blackfan anemia (DBA) is a rare congenital disorder presenting remarkable phenotypic overlap with other inherited bone marrow failure syndromes, making differential diagnosis challenging and its confirmation often reached with great delay.

By whole exome sequencing, we unraveled the presence of pathogenic variants affecting genes already known to be involved in DBA pathogenesis (*RPL5* and *RPS19*) in three patients with otherwise uncertain clinical diagnosis, and provided new insights on DBA genotype-phenotype correlations. Remarkably, the *RPL5* c.482del frameshift mutation has never been reported before, whereas the *RPS19* c.3G>T missense mutation, although previously described in a 2-month-old DBA patient without malformations and refractory to steroid therapy, was detected here in the mosaic state in different bodily tissues for the first time in DBA patients.

© 2017 Elsevier Inc. All rights reserved.

1. Introduction

Diamond-Blackfan anemia (DBA, OMIM 105650) is a rare (5–7 cases per million live births) inherited bone marrow failure syndrome (IBMFS), a group of genetic disorders with great phenotypic overlap, whose diagnosis is often challenging but essential for precise clinical management [1,2].

DBA is characterized by isolated normochromic and usually macrocytic anemia, reticulocytopenia and decreased number of erythroid precursors in otherwise normocellular bone marrow [3]. Although anemia is the most prominent feature, DBA is also characterized by growth retardation and congenital malformations, which are present in approximately half of the patients; additionally, DBA patients have a predisposition to develop malignancies [4].

Penetrance is incomplete and clinical expressivity widely variable, and within affected families some individuals may exhibit mild or absent anemia, with only very subtle indications of erythroid abnormalities. Importantly, it is argued that some DBA patients who present with craniofacial malformations and absent or very mild hematological abnormalities are underdiagnosed. The vast majority (~90%) of affected individuals typically present symptoms during the first year of life or in early childhood, even if non-classical mild phenotypes may not be diagnosed until later in life [5,6]. Although most DBA cases are sporadic, about 20% of patients have a positive family history with autosomal dominant inheritance [7]. Except for the rare germline *GATA1* (Xp11.23, OMIM 300835) and *TSR2* (Xp11.22, OMIM 300946) mutations, inherited in an X-linked manner [8,9], most of the DBA causative mutations have been identified in genes encoding ribosomal proteins (RP) of the 40S or 60S ribosomal subunits [10–18]. Nevertheless, the

underlying molecular defect remains unknown in approximately half of DBA patients currently analyzed by conventional screening techniques (*e.g.* direct sequencing), drawing attention to the need for high-throughput sequencing approaches [19,20].

Although dominant negative effects of mutant RPs, particularly in the case of *RPS19*, have been implicated by some missense coding mutations and demonstrated in model systems [21], a generally recognized pathogenic hypothesis implies RPs haploinsufficiency by defective ribosome biogenesis and pre-rRNA maturation [22,23], leading to apoptosis of erythroid progenitor cells [24,25]. Moreover, defects in extra-ribosomal proteins, such as transcription factors required for erythroid differentiation, might also contribute to the overall complexity of observed phenotypes [26].

The highly variable clinical expression of DBA, together with the absence of reliable biochemical markers, make identification of the causative mutation essential to establish a definitive diagnosis of DBA. Moreover, identification of asymptomatic or pauci-symptomatic carriers is mandatory when potential donors of hematopoietic stem cells are evaluated within first-degree relatives, and prenatal diagnosis may be requested for families with severely affected children. Finally, the definition of the molecular defect might be useful for gene therapy to modulate the expression of mutated RP genes and overcome the underlying bone marrow failure [27,28].

In this study, we performed whole exome sequencing (WES) in two families with uncertain clinical diagnosis and provided further evidence that high-throughput sequencing technologies may strongly contribute to the proper classification of patients with inherited bone marrow failure syndromes, in agreement with previous reports [29–31].

2. Material and methods

2.1. Clinical reports

2.1.1. Family A

The index case, a 4-year-old boy of Italian descent, was born after 36 weeks of gestation by caesarean section. Pregnancy was complicated by intrauterine growth restriction (IUGR) and oligohydramnios. At birth, weight was 1875 g (≤10th centile), length 44 cm (10th centile) and head circumference 31 cm (10th centile). The APGAR score was 8 and 8 at 1′ and 5′, respectively. The baby showed hypotonia, cyanosis, systolic heart murmur and heart rate above 100 bpm, requiring oxygen-therapy. Hematological evaluation revealed a hemoglobin level of 9.4 g/dl, RBC $3.30 * 10^{12}$/L, Ht 28.6%, borderline MCV (86.7 fl), while normal MCH (28.5 pg), MCHC (32.9 g/dl) and reticulocyte count ($29.40 * 1000$/mm^3). Erythroblasts were not present in the bloodstream, and routine biochemical analytes were in the normal range. When heas 10-day-old, clinical examination revealed cleft palate. At the age of 2 months a cerebral ultrasound investigation showed ventriculomegaly, enlargement of the subarachnoid spaces, plagiocephaly, and hydrocephalus. Abdominal ultrasonography detected renal calculosis with significant pyelic dilatation. Repeated hematological assessments confirmed severe anemia and mild neutropenia. The patient was initially diagnosed with suspected Shwachman-Diamond syndrome (SDS, OMIM 260400), thereafter discarded since the patient did not develop any of the most peculiar features of this syndrome, such as exocrine pancreatic insufficiency, pancreatic lipomatosis and metaphyseal chondrodysplasia.

The patient achieved autonomous walking at 15 months, when the clinical examination revealed macrocephaly (75th centile), slightly low-set ears, anteverted nares, clinodactyly of the 5th finger, broad toes, distal phalangeal hypoplasia, and high arched feet. At 4 years and 9 months, the patient additionally showed hair with widow's peak, small ears with hypoplastic helices, deep-set eyes, downward-slanting palpebral fissures, and small mouth (Fig. 1). X-rays of hands and feet revealed severe syndactyly of the feet, hypoplasia of the distal phalanges of the 4th and 5th fingers and of the 2nd and 3rd toes, as well as bilateral

aplasia of the intermediate and distal phalanges of the 4th and 5th toes, and bilateral pes cavus. The cleft palate was corrected surgically and tympanostomy tubes were placed because of recurrent episodes of airway infections and otitis media.

The family history revealed that the patient's mother (39 years old) suffered from anemia and mild leucopenia since she was 10 years old and was investigated for MDS at the age of 28. The bone marrow biopsy demonstrated hypocellularity, delayed cellular maturation, and an abnormal lymphoid component with abundant reactive lymphocytes. The immunohistochemical characterization detected an increased number of CD3 + cells, with normal CD4+/CD8+ T cell ratio, and low rate of CD57 + cells. The bone marrow karyotyping was 46,XX with any chromosomal alteration. Abdominal ultrasonography demonstrated hepatomegaly with otherwise conserved hepatocellular architecture. The clinical examination revealed small head circumference (52 cm, 3rd centile), deep-set eyes, anteverted nares, nasal septum extended below alae nasi, short columella, and hallux valgus.

The proband's sister was born by caesarean section after 34 weeks of gestation complicated by IUGR, oligohydramnios, and cardiotocographic anomalies. At birth, weight was 1225 g (<3rd centile), length 37 cm (3rd centile), and head circumference 29.2 cm (3rd–10th centile). APGAR score was 9 at 1′ and 9 at 5′. She was admitted to a Neonatal Intensive Care Unit at the first day of life, because of prematurity and profound anemia (blood count not available). In the third month of life she presented neutropenia and RSV-related bronchiolitis, while severe anemia was treated with blood transfusions. She achieved head control at 4 months and first autonomous steps at 12 months, but did not pronounce any words until 18 months. Physical examination at 17 months revealed growth retardation, with height 73 cm (<3rd centile), and weight 7900 g (<3rd centile). She presented peculiar dysmorphic features: hair with widow's peak, pinched face, deep-set eyes, ocular hypertelorism, epicanthus inversus, low nasal bridge, cutaneous syndactyly of 4th and 5th fingers, bilateral camptodactyly and clinodactyly of the 5th fingers, broad hallux, and hypoplasia and syndactyly of the 4th–5th toes, especially on left foot (Fig. 1).

The 40-year-old patient's father only suffered from hypothyroidism treated with synthetic thyroid hormone levothyroxine.

2.1.2. Family B

The patient, a 2-year-old female child of Serbian origin, was referred to our Hospital for congenital anemia and neutropenia with the hypotheses either of Fanconi anemia (FA, OMIM 227650) or dyskeratosis congenita (DC, OMIM 224230). Her past medical history reported she was born after an uneventful pregnancy (birth weight: 3400 g) but, immediately after the delivery, she presented respiratory failure, requiring mechanical ventilation. Blood tests persistently revealed severe hyporigenerative anemia and mild neutropenia. Direct antiglobulin test, bilirubin and index of hemolysis were all negative. Bone marrow aspirate and trephine demonstrated very poor cellularity for age, marked erythroid hypoplasia and reduced number of megakariocytes. Myeloid precursors were normally represented in the different maturative stages. The karyotype revealed a normal female chromosomal asset (46, XX).

In the country of origin of the patient, DEB test was performed on both skin fibroblasts and blood cells with discordant results (positive on fibroblasts and negative on blood), while we confirmed no chromosome breakage on peripheral blood. On clinical examination, the patient did not exhibit neither craniofacial dysmorphisms nor other physical abnormalities. The liver biopsy showed hepatic siderosis and fibrosis, associated with increased aminotransferase levels, requiring iron chelation therapy with deferoxamine. The severe iron overload was confirmed by SQUID biosusceptometry. Moreover, further focused examinations, such as cardiac and abdominal ultrasonography, did not reveal anomalies involving heart, kidney and urinary tract. External genitalia were normal at the physical examination.

RPL5 c.482del; p.Gly161Valfs*3 (Family A)
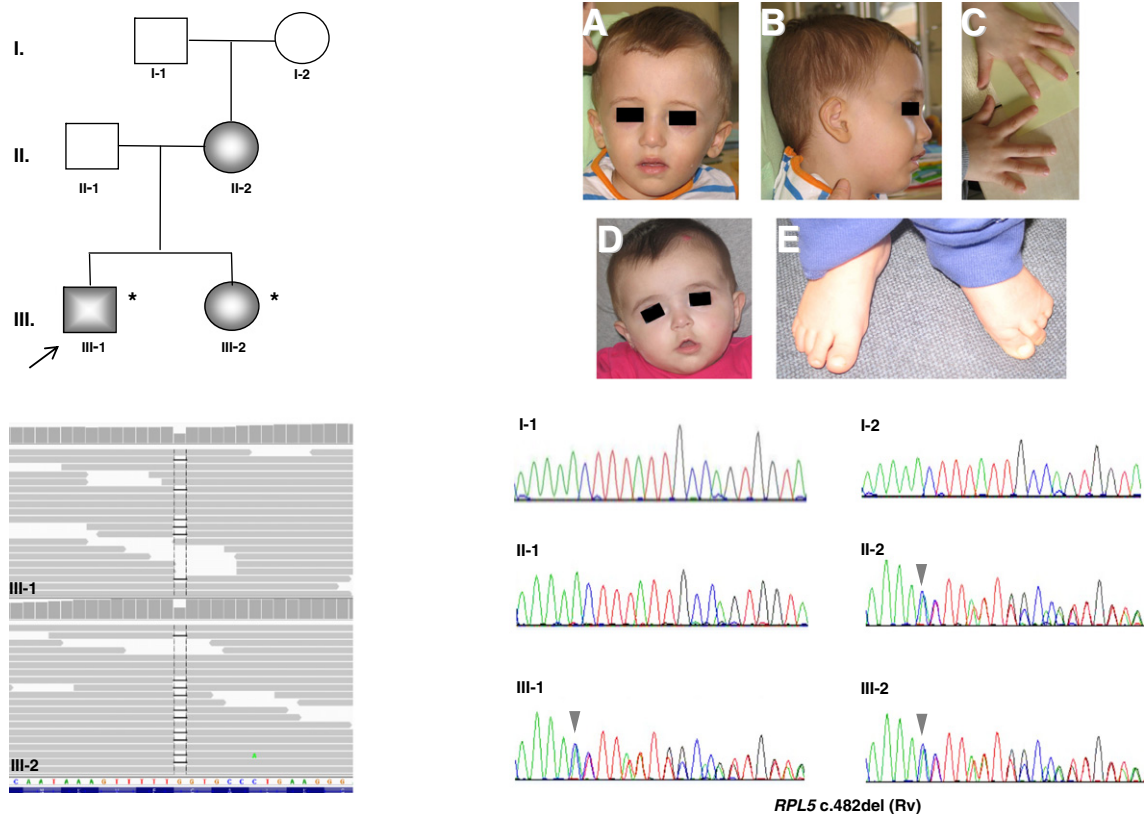
Fig. 1. Frameshift mutation in *RPL5* (c.482del) in patients III-1 and III-2 (family A). *Top panel* (*left*): pedigree of the family. The arrow indicates the index case. *: Subjects analyzed by whole exome sequencing (WES). *Top panel* (*right*): clinical features of patients III-1 and III-2. (A, B) Picture of patient III-1, showing transparent skin, high forehead, flattened occiput, widow's peak, deep-set eyes, downward-slanting palpebral fissures, and small mouth. (C) Hands of patient III-1. The boy presented short 5th fingers, especially at the right, mild clinodactyly, and apparently short distal phalanges. (D) Picture of patient III-2 at age 7 months, showing pale transparent skin, high forehead with hemangioma at the left, widow's peak, ocular hypertelorism, mild epicanthus inversus, deep-set eyes, low nasal bridge, and "tented" small mouth. (E) Patient III-2's feet with cutaneous syndactyly of digits IV–V (especially on left foot), broad halluces, and hypoplasia of the distal phalanges (mostly of 4th and 5th toes at the left). Written informed consent was obtained for both patients. *Bottom panel* (*left*): detailed view of individual sequencing reads (horizontal grey bars), as visualized by Integrative Genomics Viewer (IGV). The medium coverage for *RPL5* was 54.85× (III-1) and 61.11× (III-2). *Bottom panel* (*right*): sequence electropherograms of the *RPL5* (NM_000969.3) c.482del heterozygous frameshift mutation (indicated by the arrowhead).

Steroid therapy was started about four months after hospitalization because of progressive RBC transfusion dependence. The patient presented only a partial and provisional response with reduction of transfusion requirement, but without substantial improvement. Steroid treatment was progressively discontinued and after a few months she presented respiratory difficulties because of Rhinovirus-related bronchiolitis that deteriorated her clinically stable breathing disorder (interstitial lung disease), as demonstrated by HRCT (High Resolution Computed Tomography). Considering enduring RBC transfusion dependence and mild neutropenia (ANC < 1000/µL) after discontinuation of prednisone, the patient was retained eligible for hematopoietic stem cell transplantation (HSCT). She was an only child and thus HLA-matched unrelated donor was found in the International Bone Marrow Donor Registry (IBMDR). The patient underwent allogeneic HSCT at the age of 2 years and 4 months, with only limited complications. Neutrophil and platelet engraftment were reached quickly, at day +19 and +22, respectively. A coronavirus-related bronchiolitis requiring high flow oxygen supply was observed at day +12, completely resolved within 2 weeks. At day +45 she presented mild acute cutaneous Graft-*versus*-Host Disease (GvHD), treated with a brief course of systemic steroid therapy.

The parents of the index case, both of Serbian origin, were healthy and did not present any sign or symptom related to IBMFS. After molecular diagnosis, patient's anamnesis was carefully re-evaluated and considered consistent with the DBA etiology.

2.2. Genetic analysis

2.2.1. Whole exome sequencing (WES)

Genomic DNA (~3 µg) was extracted from peripheral blood samples, by using the QIAamp DNA Blood Mini Kit (Qiagen, Hilden, Germany). Library preparation was performed as previously reported [32] by using the SureSelect Human All Exon v5 target enrichment kit (Agilent Technologies). Sequencing was performed on HiSeq 2500 by using a Paired-End 100 bp protocol (Illumina, San Diego, CA, USA). Reads were aligned against the reference human genome sequence (GRCh37/hg19) by using the BWA-mem software package v0.7.12.1 PCR duplicates were filtered out by Picard v1.137 (http://picard. sourceforge.net) and the GATK v3.1 suite was used to locally realign around inferred Insertion/Deletions (InDels) and recalibrate base qualities scores.2 Single Nucleotide Variants (SNVs) and InDels were called using GATK Unified Genotyper. ANNOVAR3 was used to annotate genomic variants for public databases such as RefSeq (http://www.ncbi.nlm. nih.gov/RefSeq), dbSNP144 and dbNSFP (version 2.9.1) [33]. The latter consists in a resource of pre-computed genomic variants score (*e.g.* MutationTaster, SIFT, PolyPhen2) based on their probability to alter protein structure and functionality. Computational estimation of pathogenicity was used for prioritization of variants.

In our data analysis, we firstly focused on genes already associated with the most common IBMFS (Supplementary Table S1). Then, we excluded variants reported in 1000 Genome Project, ExAC (Exome

Aggregation Consortium) and National Heart, Lung and Blood Institute (NHLBI) Exome Sequencing Project (ESP) databases, as well as in our in-house database (composed of approximately 200 individuals), with a population frequency above 1%, and affecting non-synonymous exonic, or splice site (beyond 30 bp of exon/intron boundaries) regions. In addition, we checked for the presence of potential insertions or deletions by using the EXCAVATOR tool [34].

2.2.2. Sanger sequencing

All PCR reactions were carried out with the AmpliTaq Gold Polymerase Kit (Life Technologies, Foster City, CA, USA) in a final a final volume of 25 μL containing 50 ng of genomic DNA, Gold Buffer 1×, MgCl$_2$ 1.5 mM, dNTPs 0.2 mM, 1 U of AmpliTaq Gold DNA Polymerase and 10 pmol of both forward and reverse primers. DNA samples were denatured at 95 °C for 5 min and then amplified for 35 cycles as follows: 95 °C for 30 s, annealing at variable annealing temperature (Supplementary Table S2) for 30 s, 72 °C for 30 s; and final extension at 72 °C for 7 min. Sequencing reactions were performed using the BigDye Terminator v3.1 Cycle Sequencing Kit on a 3730 DNA Analyzer (Applied Biosystems).

2.2.3. Pyrosequencing

PCR reactions were carried out by using the following primers: 5′-TGTGTTCACATGCTTGACTTTC-3′ (forward), 5′ biotin-TGCTGGTTCAC GTCTTTTACA-3′ (reverse). Samples were denatured at 94 °C for 5 min and amplified for 35 cycles consisting of 94 °C for 45 s, 58 °C for 45 s, 72 °C for 1 min, and a final elongation at 72 °C for 5 min. The 65-bp PCR product was then analyzed by using the PyroMark Vacuum Prep Workstation (Qiagen), as previously described [35]. The primed single-stranded DNA template was subjected to real-time sequencing by using the following primer: 5′-GCTTGACTTTCTCCCTC-3′. Pyrosequencing analysis was carried out using PyroMark Q24 Instrument, and quantification of mutant vs wild-type alleles was calculated by PyroMarkQ24 software (Qiagen).

2.2.4. Array comparative genomic hybridization (Array-CGH)

Molecular karyotyping was performed on DNA samples extracted from patient's peripheral blood by using a whole-genome 180 K Agilent array (Human Genome CGH Microarray, Agilent Technologies, Santa Clara, CA, USA), as we previously reported [36]. Data were analyzed by using the Agilent Genomic Workbench Standard Edition 6.5.0.58. All genomic positions were reported according to the human genome assembly (GRCh37/hg19).

2.2.5. Ethical approval and consent

The study has been carried out in accordance with the research rules of our institutional ethical committee on human experimentation and written informed consents were obtained from all the patients or their parents.

3. Results

3.1. Family A

The index case (III-1) presented symptoms suggestive of DBA, but the clinical data were not sufficient and univocal to definitively establish a proper diagnosis (e.g. borderline MCV values). The array-CGH analysis revealed a small deletion on Xq13.3, spanning about 54 Kb (chrX:74,772,380–74,826,260, GRCh37/hg19), in the proband (Supplementary Fig. S1A). This chromosomal alteration, not reported in the Database of Genomic Variants (http://dgv.tcag.ca), was located within a region devoid of genes and the closest coding gene (~29 Kb), ZDHHC15 (chrX:74,588,262–74,743,337, GRCh37/hg19), was associated with a different phenotype (severe X-linked mental retardation, seizures and early childhood obesity, OMIM 300577) and, thus, not considered as pathogenic [37]. Moreover, Sanger sequencing analysis of the RPS19 gene, which accounts for approximately 25% of DBA cases [38], failed to

Table 1
List of candidate variants in Diamond-Blackfan Anemia (DBA), Fanconi Anemia (FA) and Dyskeratosis Congenita (DC)-associated genes detected in families A and B. RPL5 and RPS19 genes segregated with the disease in the two families. SLX4, FANCA, ATR and RTEL1 variants in family B were discarded because of the heterozygous state or overall neutral effect. TERT c.835G>A change was reported in ClinVar but was shown not to segregate with the disease [46]. The presence of compound heterozygous mutations was also excluded. PolyPhen2 and SIFT predictions were only available for non-synonymous polymorphisms or missense mutations. MAF: minor allele frequency; AD: autosomal dominant; AR: autosomal recessive.

Family	Gene	Locus	Genomic position (GRCh37/hg19)	HGVS annotation	Disease	dbSNP	SIFT	Mutation taster	PolyPhen2	Inheritance	Mutation status
A	RPL5	1p22.1	chr1:93301903delG	NM_000969.3:c482del	DBA			Disease causing		AD	Heterozygous
B	RPS19	19q13.2	chr19:42364847G>T	NM_001022.3:c3G>T	DBA	rs138938035 (MAF: 0.667%)	Disease causing	Disease causing	Probably damaging	AD	Heterozygous
B	SLX4	16p13.3	chr16:3632609C>T	NM_032444.2:c5239G>A	FA	rs201214017 (MAF: 0.046%)	Tolerated	Polymorphism	Possibly damaging	AR	Heterozygous
B	FANCA	16q24.3	chr16:89836302G>A	NM_000135.2:c2447C>T	FA	rs756082739 (MAF: 0.008%)	Disease causing	Polymorphism	Benign	AR	Heterozygous
B	ATR	3q23	chr3:142278201T>C	NM_001184.3:c1624A>G	FA	rs200491706 (MAF: 0.013%)	Tolerated	Polymorphism	Possibly damaging	AR	Heterozygous
B	TERT	5p15.33	chr5:1294166C>T	NM_198253.2:c835G>A	DC	rs61748181 (MAF: 0.958%)	Tolerated	Disease causing	Probably damaging	AR, AD	Heterozygous
B	RTEL1	20q13.33	chr20:62325833C>A	NM_032957.4:c3173C>A	DC	rs115610405 (MAF: 0.899%)	Tolerated	Polymorphism	Possibly damaging	AR, AD	Heterozygous

detect any causative variant. Subsequently, WES analysis was performed in individuals III-1 and III-2. Our filtering criteria were satisfied by only one heterozygous frameshift mutation (NM_000969.3:c.482del; NP_000960.2:p.Gly161Valfs*3), in the exon 5 of the *RPL5* gene of both siblings (Fig. 1). This loss of function (LoF) mutation, affecting a highly conserved position (PhyloP:4.24; PhastCons:1.00), was subsequently validated by traditional Sanger sequencing approach in DNA samples from available family members to determine whether the candidate variant co-segregated with the DBA phenotype within the pedigree. Parental DNA examination revealed that the mutation was inherited from the mother. Further molecular analysis of the maternal grandparents, who did not show any symptom, confirmed that the mutation occurred *de novo* in the patients' mother (Fig. 1). The variant created a frameshift at codon 161 resulting in a premature stop codon two positions downstream and, according to *in silico* predictions, the mRNA produced was expected to be degraded through nonsense mediated mRNA decay (NMD).
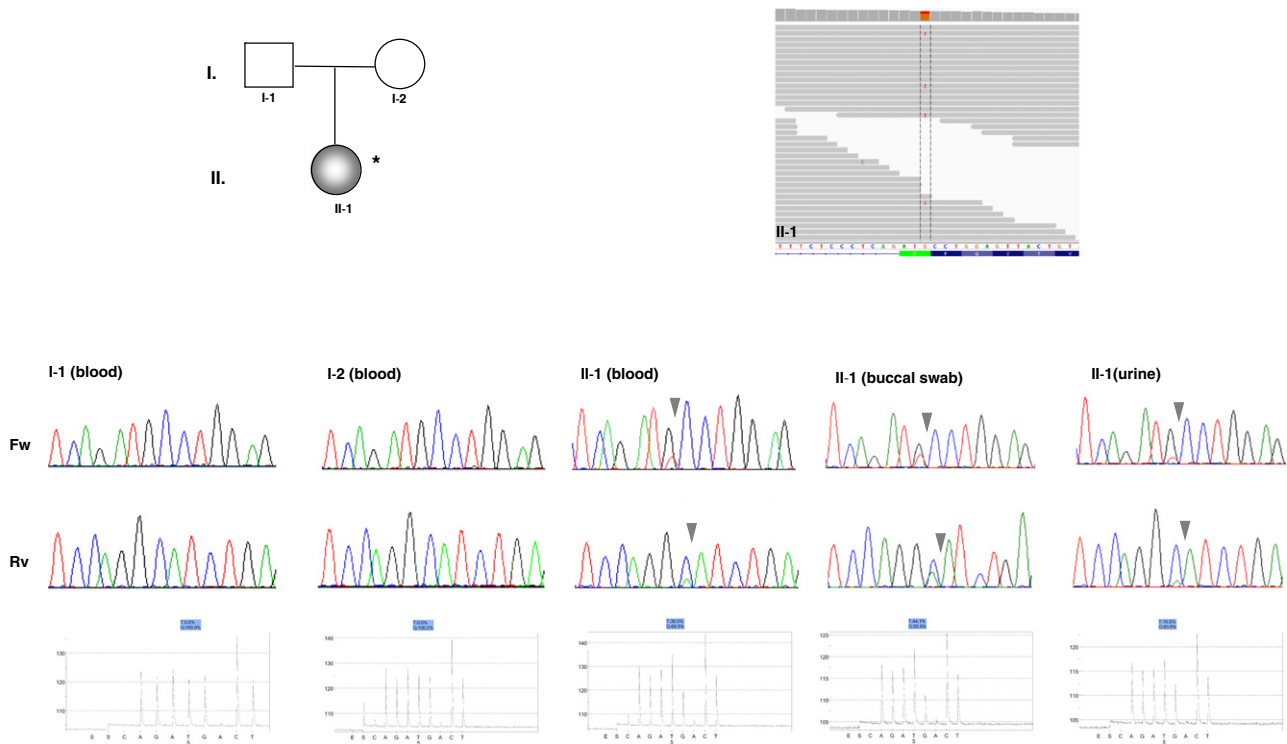
3.2. Family B

In this family, the clinical diagnosis was initially uncertain, due to the phenotypic overlap frequently observed among the IBMFS. Accordingly, the NGS data were filtered considering different panels of genes involved in these hematologic diseases (Supplementary Table S1). The preliminary filtering process for FA and DC-associated genes (according to the initial clinical diagnosis) did not unveil any disease-causing variant, either for predicted *in silico* overall neutral effect or for inconsistent inheritance pattern (Table 1). On the contrary, after filtering of variants for DBA-associated genes, we obtained a unique heterozygous missense variant (NM_001022.3:c.3G>T; NP_001013.1:p.Met1?), in the exon 2

of *RPS19* of patient II-1 (Fig. 2). This substitution, leading to the loss of the highly conserved translation initiation codon (PhyloP:5.13; PhastCons:1.00), was predicted to be damaging by almost all the *in silico* tools (Table 1). An alternative in-frame start codon was not present around the mutated position, as assessed by ORF Finder and StarORF, although the contribution of alternative translation initiation signals (TISs) might also be considered [39]. Moreover, this variant was reported in HGMD (#CM005392) and dbSNP142 (rs138938035, with a frequency of the minor T allele of 0.7% in the population), and previously reported as causative [40]. Other two missense mutations in the initial methionine codon (c.1A>G and c.2T>A) were described in large cohorts of DBA patients without malformations, growth retardation and steroid response [24,41]. As assessed by IGV visual inspection, the c.3G>T transversion showed variation in allele fraction in our patient (G:70%, T:30% with read depth of 84×), thus suggesting mosaicism. This unbalanced allelic ratio was further confirmed by both Sanger sequencing and quantitative pyrosequencing assays in blood as well as buccal swab and urine specimens (Fig. 2 and Supplementary Fig. S2). While a *de novo* germline mutation is typically associated with an allelic ratio of approximately 50%, the observed lower ratio suggested that the mutation more likely arose during embryogenesis. Accordingly, the mutation was absent in the parental DNA samples. Finally, any pathogenic copy number variation (CNV) was detected in the proband, as assessed by the EXCAVATOR's data analysis (Supplementary Fig. S1B).

4. Discussion

In contrast to patients that harbor mutations of *RPS19* and *RPL11* genes, mutations in *RPL5* have generally been associated with a more severe phenotype including multiple physical (craniofacial, thumb,

RPS19 c.3G>T; p.Met1? (Family B)

Fig. 2. Mosaic missense mutation in *RPS19* (c.3G>T) in patient II-1 (family B). *Top panel* (*left*): pedigree of the family. *: Patient analyzed by whole exome sequencing (WES). In subject II-1 blood was collected before bone marrow transplantation. *Top panel* (*right*): Detailed view of individual sequencing reads (horizontal grey bars), as visualized by Integrative Genomics Viewer (IGV). The medium coverage for *RPS19* was 83.10×. *Bottom panel*: sequence electropherograms and pyrograms of the *RPS19* (NM_001022.3) c.3G>T mosaic missense mutation by bidirectional dideoxy sequencing and pyrosequencing, respectively, in different specimens. The figures are representative of three independent experiments performed in triplicate on three different DNA extractions. Heterozygous mutations are indicated by arrowheads. Fw: forward strand; Rv: reverse strand. Parents of patient II-1 denied permission to publish pictures.

heart) abnormalities, SGA (Small for gestational age), and short stature [14,42,43]. Moreover, it has been suggested that *RPL5* mutations might have a more profound impact on fetal development than mutations in other RP genes, primarily *RPS19* [15,19,44]. In accordance with these findings, patient III-1 (family A) showed different physical anomalies, as well as intrauterine growth restriction (IUGR). On the other hand, physical anomalies were not present in the affected member of family B, carrying a *RPS19* mutation.

Up to now, *RPL35A* has been considered the gene most frequently associated with genitourinary malformations among DBA patients [13], but the fact that patient III-1 in family A showed renal calculosis and pyelic dilatation further underlines the need for large association studies. On the other hand, the results of the molecular analysis in family B strengthen the influence of the genotype on the treatment. Indeed, it has been previously reported that patients with *RPS19* mutations display a diminished long-term prognosis and poor response to steroids [12], as we documented in patient II-1.

In summary, we identified two pathogenic variants in *RPL5* and *RPS19* genes, one of which never reported before (*RPL5* c.482del), broadening the spectrum of DBA clinical phenotypes. Moreover, the missense c.3G>T mutation, even if previously reported, was here detected in a mosaic state. To our knowledge, mosaic point mutations have never been reported in DBA patients. Previously, Farrar et al. [45] described three DBA individuals with mosaic copy loss on chromosomes 3q and 15q, containing two well-established DBA genes, *RPL35A* (3q29) and *RPS17* (15q25.2). Interestingly, the two patients with low-level mosaicism experienced a spontaneous remission of DBA in the second decade of life, whereas the subject with a higher fraction of mosaicism remained transfusion-dependent. These findings suggest that the fraction of blood mosaicism may correlate with the prognosis and may also impact on the clinical outcome of our young patient with a mosaic *RPS19* missense mutation.

In conclusion, this study further strengthens the fundamental role of whole exome sequencing in the differential diagnosis of IBMFS, as well as in the achievement of a personalized medicine approach.

Conflict of interest statement

The authors declare that there is no conflict of interest.

Authors' contribution

EE and AV conceived the experiments and interpreted the results. EE reviewed all experimental data and wrote the manuscript. TM, AW, and MR collected clinical data. MC carried out the array-CGH experiments. EB and TV performed pyrosequencing assays. MZ and PS contributed to the final revision of the article. OZ conceived the work, participated in its design and finally revised the manuscript. All authors approved the final manuscript.

Acknowledgements

Appendix A. Supplementary data

Supplementary data to this article can be found online at http://dx.doi.org/10.1016/j.bcmd.2017.03.002.

References

[1] I. Dokal, T. Vulliamy, Inherited bone marrow failure syndromes, Haematologica 95 (8) (2010) 1236–1240.

[2] Michael Y. Zhang, B. Siobán, et al., Genomic analysis of bone marrow failure and myelodysplastic syndromes reveals phenotypic and diagnostic complexity, Haematologica 100 (1) (2015) 42–48.

[3] M.F. Campagnoli, E. Garelli, P. Quarello, et al., Molecular basis of Diamond-Blackfan anemia: new findings from the Italian registry and a review of the literature, Haematologica 89 (4) (2004) 480–489.

[4] A. Vlachos, P.S. Rosenberg, E. Atsidaftos, B.P. Alter, J.M. Lipton, Incidence of neoplasia in Diamond Blackfan anemia: a report from the Diamond Blackfan anemia registry, Blood 119 (16) (2012) 3815–3819.

[5] P. Farruggia, P. Quarello, E. Garelli, O. Paolicchi, G.B. Ruffo, L. Cuccia, S. Cannella, G. Bruno, P. D'Angelo, The spectrum of non-classical Diamond-Blackfan anemia: a case of late beginning transfusion dependency associated to a new RPL5 mutation, Pediatr. Rep. 4 (2) (2012) e25.

[6] E. Flores Ballester, J.J. Gil-Fernández, M. Vázquez Blanco, J.M. Mesa, García J. de Dios, A.T. Tamayo, C. Burgaleta, Adult-onset Diamond-Blackfan anemia with a novel mutation in the exon 5 of RPL11: too late and too rare, Clin. Case Rep. 3 (6) (2015) 392–395.

[7] R. Wang, K. Yoshida, T. Toki, et al., Loss of function mutations in RPL27 and RPS27 identified by whole-exome sequencing in Diamond-Blackfan anaemia, Br. J. Haematol. 168 (6) (2015) 854–864.

[8] V.G. Sankaran, R. Ghazvinian, R. Do, et al., Exome sequencing identifies GATA1 mutations resulting in Diamond-Blackfan anemia, J. Clin. Invest. 122 (7) (2012) 2439–2443.

[9] K.W. Gripp, C. Curry, A.H. Olney, et al., Diamond-Blackfan anemia with mandibulofacial dystostosis is heterogeneous, including the novel DBA genes TSR2 and RPS28, Am. J. Med. Genet. A 164A (9) (2014) 2240–2249.

[10] H.T. Gazda, A. Grabowska, L.B. Merida-Long, et al., Ribosomal protein S24 gene is mutated in Diamond-Blackfan anemia, Am. J. Hum. Genet. 79 (6) (2006) 1110–1118.

[11] R. Cmejla, J. Cmejlova, H. Handrkova, J. Petrak, D. Pospisilova, Ribosomal protein S17 gene (RPS17) is mutated in Diamond-Blackfan anemia, Hum. Mutat. 28 (12) (2007) 1178–1182.

[12] M.F. Campagnoli, U. Ramenghi, M. Armiraglio, et al., RPS19 mutations in patients with Diamond-Blackfan anemia, Hum. Mutat. 29 (7) (2008) 911–920.

[13] J.E. Farrar, M. Nater, E. Caywood, et al., Abnormalities of the large ribosomal subunit protein, Rpl35a, in Diamond-Blackfan anemia, Blood 112 (5) (2008) 1582–1592.

[14] H.T. Gazda, M.R. Sheen, A. Vlachos, et al., Ribosomal protein L5 and L11 mutations are associated with cleft palate and abnormal thumbs in Diamond-Blackfan anemia patients, Am. J. Hum. Genet. 83 (6) (2008) 769–780.

[15] R. Cmejla, J. Cmejlova, H. Handrkova, J. Petrak, K. Petrtylova, V. Mihal, J. Stary, Z. Cerna, Y. Jabali, D. Pospisilova, Identification of mutations in the ribosomal protein L5 (RPL5) and ribosomal protein L11 (RPL11) genes in Czech patients with Diamond-Blackfan anemia, Hum. Mutat. 30 (3) (2009) 321–327.

[16] L. Doherty, M.R. Sheen, A. Vlachos, et al., Ribosomal protein genes RPS10 and RPS26 are commonly mutated in Diamond-Blackfan anemia, Am. J. Hum. Genet. 86 (2) (2010) 222–228.

[17] P. Quarello, E. Garelli, A. Brusco, A. Carando, C. Mancini, P. Pappi, L. Vinti, J. Svahn, I. Dianzani, U. Ramenghi, High frequency of ribosomal protein gene deletions in Italian Diamond-Blackfan anemia patients detected by multiplex ligation-dependent probe amplification assay, Haematologica 97 (12) (2012) 1813–1817.

[18] M. Landowski, M.F. O'Donohue, C. Buros, et al., Novel deletion of RPL15 identified by array-comparative genomic hybridization in Diamond-Blackfan anemia, Hum. Genet. 132 (11) (2013) 1265–1274.

[19] G. Gerrard, M. Valgañón, H.E. Foong, et al., Target enrichment and high-throughput sequencing of 80 ribosomal protein genes to identify mutations associated with Diamond-Blackfan anaemia, Br. J. Haematol. 162 (4) (2013) 530–536.

[20] J. Zhang, P. Barbaro, Y. Guo, et al., Utility of next-generation sequencing technologies for the efficient genetic resolution of haematological disorders, Clin. Genet. 89 (2) (2016) 163–172.

[21] E.E. Devlin, L. Dacosta, N. Mohandas, G. Elliott, D.M. Bodine, A transgenic mouse model demonstrates a dominant negative effect of a point mutation in the RPS19 gene associated with Diamond-Blackfan anemia, Blood 116 (15) (2010) 2826–2835.

[22] V. Choesmel, S. Fribourg, A.H. Aguissa-Touré, et al., Mutation of ribosomal protein RPS24 in Diamond-Blackfan anemia results in a ribosome biogenesis disorder, Hum. Mol. Genet. 17 (9) (2008) 1253–1263.

[23] J.E. Farrar, P. Quarello, R. Fisher, et al., Exploiting pre-rRNA processing in Diamond Blackfan anemia gene discovery and diagnosis, Am. J. Hematol. 89 (10) (2014) 985–991.

[24] I. Boria, E. Garelli, H.T. Gazda, et al., The ribosomal basis of Diamond-Blackfan anemia: mutation and database update, Hum. Mutat. 31 (12) (2010) 1269–1279.

[25] P. Jaako, S. Debnath, K. Olsson, Y. Zhang, J. Flygare, M.S. Lindström, D. Bryder, S. Karlsson, Disruption of the 5S RNP-Mdm2 interaction significantly improves the erythroid defect in a mouse model for Diamond-Blackfan anemia, Leukemia 29 (11) (2015) 2221–2229.

[26] L.S. Ludwig, H.T. Gazda, J.C. Eng, et al., Altered translation of GATA1 in Diamond-Blackfan anemia, Nat. Med. 20 (7) (2014) 748–753.

[27] J. Flygare, K. Olsson, J. Richter, S. Karlsson, Gene therapy of Diamond Blackfan anemia CD34(+) cells leads to improved erythroid development and engraftment following transplantation, Exp. Hematol. 36 (11) (2008) 1428–1435.

[28] P. Jaako, S. Debnath, K. Olsson, et al., Gene therapy cures the anemia and lethal bone marrow failure in a mouse model of RPS19-deficient Diamond-Blackfan anemia, Haematologica 99 (12) (2014) 1792–1798.

[29] P.P. Khincha, S.A. Savage, Genomic characterization of the inherited bone marrow failure syndromes, Semin. Hematol. 50 (4) (2013) 333–347.

[30] T. Ichimura, K. Yoshida, Y. Okuno, et al., Diagnostic challenge of Diamond-Blackfan anemia in mothers and children by whole-exome sequencing, Int. J. Hematol. (2016).

[31] H. Muramatsu, Y. Okuno, K. Yoshida, et al., Clinical utility of next-generation sequencing for inherited bone marrow failure syndromes, Genet. Med. (2017). http://dx.doi.org/10.1038/gim.2016.197.

[32] A. Vetro, M. Iascone, I. Limongelli, et al., Loss-of-function FANCL mutations associate with severe Fanconi anemia overlapping the VACTERL association, Hum. Mutat. 36 (5) (2015) 562–568.

[33] X. Liu, X. Jian, E. Boerwinkle, dbNSFP v2.0: a database of human non-synonymous SNVs and their functional predictions and annotations, Hum. Mutat. 34 (9) (2013) E2393–E2402.

[34] A. Magi, L. Tattini, I. Cifola, et al., EXCAVATOR: detecting copy number variants from whole-exome sequencing data, Genome Biol. 14 (10) (2013) R120.

[35] T. Venesio, A. Balsamo, E. Errichiello, G.N. Ranzani, M. Risio, Oxidative DNA damage drives carcinogenesis in MUTYH-associated-polyposis by specific mutations of mitochondrial and MAPK genes, Mod. Pathol. 26 (10) (2013) 1371–1381.

[36] E. Errichiello, F. Novara, A. Cremante, A. Verri, J. Galli, E. Fazzi, D. Bellotti, L. Losa, M. Cisternino, O. Zuffardi, Dissection of partial 21q monosomy in different phenotypes: clinical and molecular characterization of five cases and review of the literature, Mol. Cytogenet. 9 (1) (2016) 21.

[37] M.R. Mansouri, L. Marklund, P. Gustavsson, E. Davey, B. Carlsson, C. Larsson, I. White, K.H. Gustavson, N. Dahl, Loss of ZDHHC15 expression in a woman with a balanced translocation t(X;15)(q13.3;cen) and severe mental retardation, Eur. J. Hum. Genet. 13 (8) (2005) 970–977.

[38] M. Angelini, S. Cannata, V. Mercaldo, L. Gibello, C. Santoro, I. Dianzani, F. Loreni, Missense mutations associated with Diamond-Blackfan anemia affect the assembly of ribosomal protein S19 into the ribosome, Hum. Mol. Genet. 16 (14) (2007) 1720–1727.

[39] H. Zur, T. Tuller, New universal rules of eukaryotic translation initiation fidelity, PLoS Comput. Biol. 9 (7) (2013) e1003136.

[40] U. Ramenghi, M.F. Campagnoli, E. Garelli, et al., Diamond-Blackfan anemia: report of seven further mutations in the RPS19 gene and evidence of mutation heterogeneity in the Italian population, Blood Cells Mol. Dis. 26 (5) (2000) 417–422.

[41] T.N. Willig, N. Draptchinskaia, I. Dianzani, et al., Mutations in ribosomal protein S19 gene and diamond blackfan an Diamond Blackfan anaemia in the UK: clinical and genetic heterogeneity, Blood 94 (12) (1999) 4294–4306.

[42] K.A. Orfali, Y. Ohene-Abuakwa, S.E. Ball, Diamond Blackfan anaemia in the UK: clinical and genetic heterogeneity, Br. J. Haematol. 125 (2) (2004) 243–252.

[43] D. Pospisilova, J. Cmejlova, B. Ludikova, et al., The Czech National Diamond-Blackfan Anemia Registry: clinical data and ribosomal protein mutations update, Blood Cells Mol. Dis. 48 (4) (2012) 209–218.

[44] Y. Wan, Q. Zhang, Z. Zhang, et al., Transcriptome analysis reveals a ribosome constituents disorder involved in the RPL5 downregulated zebrafish model of Diamond-Blackfan anemia, BMC Med. Genet. 9 (2016) 13.

[45] J.E. Farrar, A. Vlachos, E. Atsidaftos, H. Carlson-Donohoe, T.C. Markello, R.J. Arceci, S.R. Ellis, J.M. Lipton, D.M. Bodine, Ribosomal protein gene deletions in Diamond-Blackfan anemia, Blood 118 (26) (2011) 6943–6951.

[46] T.J. Vulliamy, A. Walne, A. Baskaradas, P.J. Mason, A. Marrone, I. Dokal, Mutations in the reverse transcriptase component of telomerase (TERT) in patients with bone marrow failure, Blood Cells Mol. Dis. 34 (3) (2005) 257–263.